LA-UR- 96- 667

CONF-960706--6

Title: RESPONSE OF A STAINLESS STEEL CYLINDER WITH ELLIPTICAL ENDS SUBJECTED TO AN OFF-CENTER BLAST LOAD

Author(s): RICK MARTINEAU
CHRISTOPHER ROMERO

Submitted to: AMERICAN SOCIETY OF MECHANICAL ENGINEERS

Los Alamos
NATIONAL LABORATORY

Form No. 836 R5
ST 2629 10/91

RESPONSE OF A STAINLESS STEEL CYLINDER WITH ELLIPTICAL ENDS SUBJECTED TO AN OFF-CENTER BLAST LOAD

Rick Martineau
Engineering Analysis Group, ESA-EA
Los Alamos National Laboratory
Los Alamos, New Mexico

Christopher Romero
Experiment & Diagnostic Design Group, DX-5
Los Alamos National Laboratory
Los Alamos, New Mexico

ABSTRACT

The response of a stainless steel cylindrical vessel with asymmetric internal blast loading is investigated by experiments, computations, and analysis. Previous research has focused on the response of cylindrical vessels for a centrally located charge. The vessel's geometry consists of a thin shell cylinder with 2:1 elliptical ends. The high explosive charge is located on the vessel's axis of symmetry and is axially offset from its geometric center. All explosives are spherical in shape and centrally initiated inside the vessel. The vessel holds the high explosive in air at ambient temperature and pressure.

Two-dimensional, Eulerian finite difference calculations from a hydrodynamic code (MESA-2D) are used to study the blast phenomenon and pressure loading on the vessel walls. The loading pulse is compared to data obtained from four experiments where several pressure transducers are positioned along the vessel's circumference. The calculated two-dimensional loading is applied to a three-dimensional explicit finite element model (DYNA-3D) to predict the structural response of the vessel. The vessel's structural response from the experimental wave interaction is recorded using strain gages, positioned along its circumference, and then compared with the finite element calculations. These results (experimental and computational) are then compared with analytical predictions and prove to correlate well at distances away from the ends. Experimental and computational results compare well at all other locations.

NOMENCLATURE

E - Youngs Modulus (psi)
R - Initial Cylinder Radius to Midsurface (in.)
$T = c_p t/R$ - Non-Dimensional Time Parameter
h - Wall Thickness of Cylinder (in.)
t - Time (sec)
u - Non-Dimensional Displacement (w/R) (Hoop Strain)
w - Outward Radial Displacement (in.)
β - Non-Dimensional Parameter
κ - Initial Velocity Ratio of Outward Radial Velocity to Plate Velocity
ν - Poisson Ratio
ρ - Mass Density (lbf-sec^2/in^4)
$c_p = [E/\rho(1-\nu^2)]^{1/2}$ - Plate Velocity (in/sec)
f_0 - Fundamental Radial Extension Mode Frequency (Hz)
I_s - Specific Impulse (psi-sec)
$V_o = I_s/\rho h$ - Outward Radial Velocity (in/sec)

1.0 INTRODUCTION

Containment of high explosions in vessels is increasingly becoming the preferred alternative for testing and disposal in the chemical and explosives manufacturing industries. Bomb disposal units currently use these vessels to transport small devices away from populated areas for safe detonation in remote locations. Several investigations have reported on the plastic response of spherical and cylindrical shells used for containment of high explosive detonations. Specifically, Baker[1], and Benham and Duffey[2] have focused on high explosive charge detonation for spherical and cylindrical vessels, respectively. Detonation of the high explosive for both systems occurs at the geometric center producing a symmetric pressure loading on the interior wall. Similarly, Proctor[3] evaluates the problem of water-filled right circular cylinders and develops basic explosion-containment relations.

The problem of asymmetric pressure loading caused by an off-center internal high explosive detonation in a cylindrical vessel is discussed in this paper. Limited study for this problem has been pursued for cylindrical vessels with capped ends. However, Belov, et. al.[4] have considered both center and off-center blast loading for spherical vessels and discuss the effects of asymmetric loading on strain rate.

The purpose of this paper is to present computational, experimental, and analytical results (away from the ends) for an off-center high explosive spherical charge detonation inside a cylindrical vessel with 2:1 elliptical ends. Computational (MESA-

2D) and experimental pressure histories are presented and compared. The computational pressure loading is then applied to a structural numerical model (DYNA-3D) and compared to experimental strain histories at various locations around the vessel. Correlation of the data is presented and summarized.

2.0 VESSEL GEOMETRY AND HIGH EXPLOSIVE CHARGE

The vessel used for the experiments and computations consists of a rolled cylindrical tube with two 2:1 elliptical ends and is fabricated using 304 Stainless Steel. This material was chosen because of its strain rate properties. The inside diameter of the vessel is 19-1/4 in. with a 3/8 in. wall thickness. The overall length of the vessel is approximately 29 in. A 2 in. pipe plug is centrally welded on the top of an elliptical end and is used to position the high explosive charge inside the vessel. The vessel is supported freely on a steel stand to minimize the effects of a rigid mount. Figure 1 shows the system in question.

The high explosive for each experiment consists of a spherical detonator surrounded by a 1/2 in. diameter ball of PETN. Composition C-4 is then molded around the PETN to increase the overall charge diameter to 1-1/2 in. This provides an overall charge weight of 0.0999 lbs. The high explosive is attached to the 2 in. pipe plug and positioned 3.87 in. below the vessel's geometric center. This location (as shown in Fig. 1) will identify the origin of the system in cylindrical coordinates.

3.0 EXPERIMENTAL PROGRAM

Four pressure transducers and four uniaxial strain gages were used in the experiments with a 2 microsecond sampling rate - see Fig. 1. Table 1 identifies the location, mounting scheme, and types of pressure transducers and strain gages. The uniaxial strain gages were mounted in a biaxial configuration to measure hoop and axial strain. The transducers were coated with a thin film of grease to help reduce the effects of heating due the high explosive thermal energy release. Transducers 1, 2, and 3 were surrounded by closed cell soft foam inside the pipe nipples for shock isolation purposes. Transducer 4, which was added after the second experiment, had no shock isolation because of its mounting scheme - see Table 1. Thus, this transducer was susceptible to vibrations from the vessel wall.

Four experiments were performed to evaluate the pressure-time loading and structural response of the vessel. The first experiment recorded data from Transducer 1, 2, & 3 and Gages 1 & 2. Transducer 3 (PVC type) separated from the vessel after the first couple of milliseconds due to the blast loading. It did, however, remain on the vessel long enough to record useful data. This transducer, therefore, was not used in subsequent experiments. The second experiment recorded data from Transducers 1 & 2 and Gages 1 & 2. Transducer 4 was added to the vessel after the second experiment. This was done primarily to verify whether or not a simpler mounting scheme would provide accurate data. Secondly, a verification of symmetric loading, with respect to Transducer 1, was expected. The third and fourth experiment recorded data from Transducers 1, 2, & 4 and Gages 1 & 2. However, data from Transducer 4 recorded too much noise to be useful and was, therefore, neglected. This noise was attributed to lack of shock isolation between the vessel and the transducer itself.

TABLE 1. Pressure Transducer & Strain Gage Information

	LOCATION (r,θ,z)	MOUNTING SCHEME	TYPE
PT No. 1	(10,180°,0)	Stainless Steel Pipe Nipple Welded to Vessel	PCB Electronics 102M164
PT No. 2	(10,0°,4.87)	Stainless Steel Pipe Nipple Welded to Vessel	PCB Electronics 102M164
PT No. 3	(10,180°,9.75)	PVC Pipe Fitting with RTV Adhesive	PCB Electronics 102M164
PT No. 4	(10,90°,0)	Rigidly Screwed onto Vessel Wall	PCB Electronics 102M164
Biaxial SG No. 1	(10,270°,0)	Directly on Vessel Wall with Epoxy Resin	BLH Electronics SNB3-16-35S9 Semiconductor Type
Biaxial SG No. 2	(10,270°,9.75)	Directly on Vessel Wall with Epoxy Resin	BLH Electronics SNB3-16-35S9 Semiconductor Type

Also, due to instrumentation failure, Transducer 1 did not record any data for the third test, but did for the fourth. Table 2 provides a synopsis of which channels recorded useful data for each experiment.

TABLE 2. Synopsis Of Recorded Data

	EXP. 1	EXP. 2	EXP. 3	EXP. 4
PT No. 1	√	√	×	√
PT No. 2	√	√	√	√
PT No. 3	√	×	×	×
PT No. 4	Not Applicable	Not Applicable	×	×
Biaxial SG No. 1	√	√	√	√
Biaxial SG No. 2	√	√	√	√

√ = Data Recorded
× = Instrumentation Failure

4.0 NUMERICAL MODELS

MESA-2D[5] was used to determine the pressure histories internal to the vessel. The geometry used to create the MESA model, as shown in Fig. 2, consists of an axisymmetric model with an offset charge. The charge consisted of both PETN and Composition C-4 high explosive and was center detonated at time t=0. Four materials were used in the code which included: PETN, Composition C-4, Los Alamos Air (SESAME EOS 5030), and 304 Stainless Steel. The cell size for the analysis was approximately 1cm x 1cm throughout the geometry. Seventeen Eulerian massless tracer particles were located inside the inner vessel wall to track the blast load. The analysis progressed from 0 to 850 microseconds.

The pressure histories obtained from the MESA model were then applied to a 304 Stainless Steel DYNA-3D[6] finite element model created with PATRAN[7] as the pre-processor. DYNA-3D is a non-linear, explicit finite element analysis tool with robust structural transient analysis capabilities. The three dimensional model includes linear shell elements and utilizes quarter symmetry as shown in Fig. 3. The support stand consists of rigid elements. A

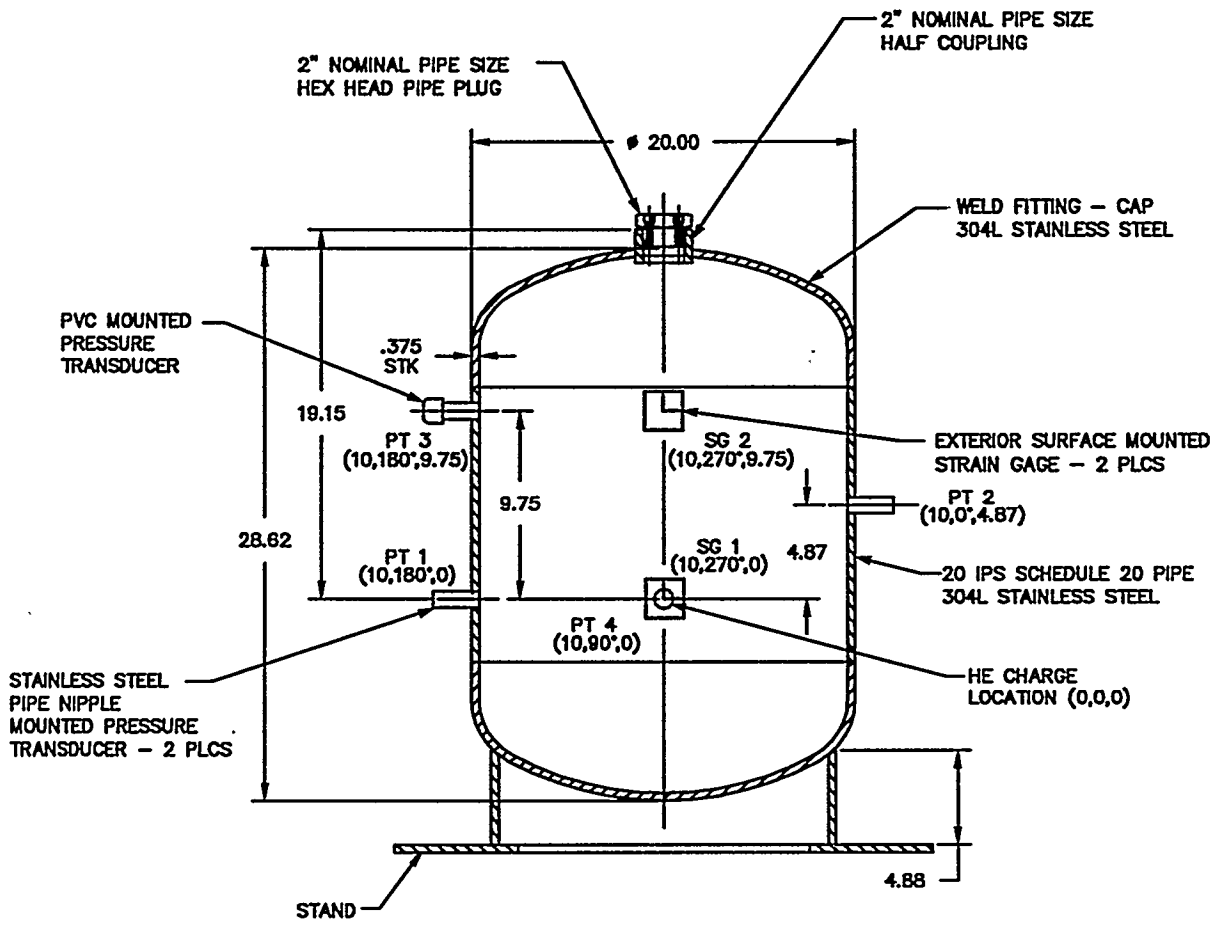

FIGURE 1. CYLINDRICAL VESSEL GEOMETRY

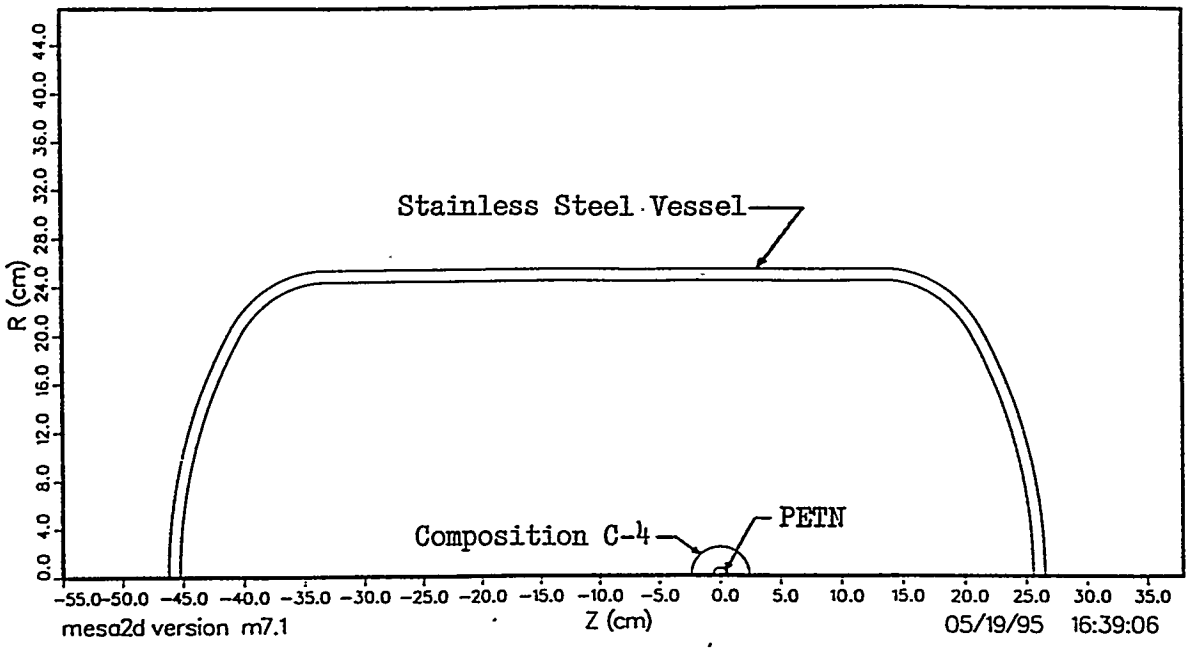

FIGURE 2. MESA-2D MODEL OF CYLINDRICAL VESSEL

contact surface is located between the support stand and the vessel. The inner surface of the vessel has seventeen axisymmetric sections for the pressure loading. These locations correspond to the tracer particle locations of the MESA model. Table 3 shows the material properties used in the model. It should be noted that the 2-in. pipe plug was not included in the model. Its weight, relative to the full vessel, is negligible and should have little effect on the vessel response. The model includes more than 3800 elements.

TABLE 3. Material Properties for the Numerical Analysis

Density	7.3896×10^{-4} lbf-sec^2/in^4
Youngs Modulus	28.0×10^6 psi
Poisson Ratio	0.291

5.0 ANALYTICAL PREDICTIONS

Analytical predictions of frequency, maximum hoop strain, and time will be used to compare with experimental and numerical results. First, the fundamental radial extension mode frequency will be determined using a formulation found in Blevins[8]. Maximum hoop strain and corresponding time will then be determined from constitutive relations developed by Duffey and Krieg[9].

Blevins shows that thin shell theory for an elastic isotropic material identifies the fundamental radial extension mode of an infinite cylinder to be:

$$f_o = \frac{1}{2\pi R}\sqrt{\frac{E}{\rho(1-\nu^2)}} \qquad (1)$$

where: f_o - *Fundamental Radial Extension Mode Frequency (Hz)*
E - *Youngs Modulus (psi)*
ρ - *Mass Density (lbf-sec^2/in^4)*
ν - *Poisson Ratio*
R - *Cylinder Radius to Midsurface (in.)*

The natural frequency of the radial extension mode of an infinite cylinder using the vessel's midsurface radius is determined to be 3300 Hz.

Duffey and Krieg have investigated the influence of the constitutive relation on the transient and final responses of impulsively loaded elastic-plastic rings and cylinders. In that study a formulation describing the elastic-plastic strain-hardening and rate sensitivity of these geometries is considered. Because the present study concerns itself with the elastic response of a cylindrical vessel, only the elastic phase formulation of Duffey and Krieg is considered. The non-dimensional displacement is given as:

$$u = \frac{\kappa}{\beta}\sin\beta T, T > 0 \qquad (2)$$

$$\kappa = \frac{V_o}{c_p} \qquad (3)$$

$$\beta = \sqrt{\frac{R}{h}\ln\left(\frac{R+h/2}{R-h/2}\right)} \qquad (4)$$

where: u - *Non-Dimensional Displacement (w/R) (Hoop Strain)*
w - *Outward Radial Displacement (in.)*

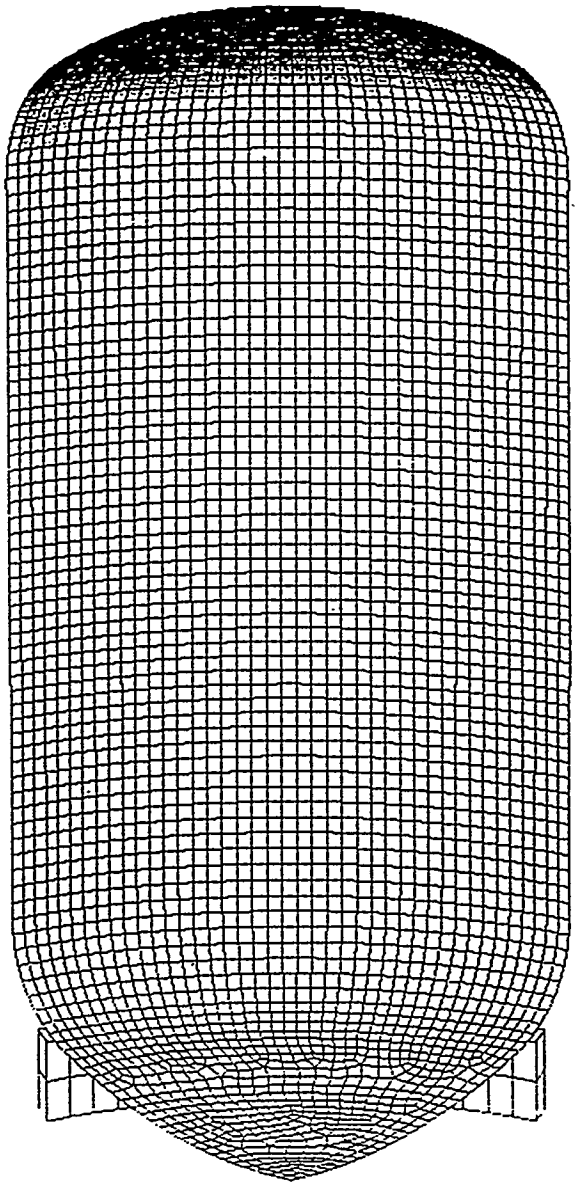

FIGURE 3. DYNA-3D FINITE ELEMENT MODEL OF CYLINDRICAL VESSEL

κ - *Initial Velocity Ratio of Outward Radial Velocity to Plate Velocity*
$V_o = I_s/\rho h$ - *Outward Radial Velocity (in/sec)*
I_s - *Specific Impulse (psi-sec)*
ρ - *Mass Density (lbf-sec^2/in^4)*
h - *Wall Thickness of Cylinder (in.)*
$c_p = [E/\rho(1-\nu^2)]^{1/2}$ - *Plate Velocity (in/sec)*
β - *Non-Dimensional Parameter*
$T = c_p t/R$ - *Non-Dimensional Time Parameter*
t - *Time (sec)*
R - *Initial Cylinder Radius to Midsurface (in.)*
E - *Youngs Modulus (psi)*

At the location (10,270°,0) on the cylinder wall (Fig. 1), Eq. (2) yields a time of 75.75 microseconds. The corresponding maximum hoop strain is, therefore, 869.2 microstrain.

6.0 RESULTS

6.1 Pressure Transducers

Figures 4 and 5 show experimental, averaged experimental, and numerical pressure histories for Transducer 1. Similarly, Figs. 6 and 7 show experimental and numerical pressure histories for Transducer 2. Figure 8 shows experimental and numerical pressure histories for Transducer 3. Recall that this transducer recorded data only for the first experiment. Transducer 4's data proved to be too noisy and was therefore neglected.

The average experimental pressure histories from all the transducers agree very well with numerical data. The initial arrival times are approximately equal and peak pressures correlate well. Any slight discrepancies between maximum pressures for the experiments can be possibly attributed to variations in the density when molding the high explosive sphere with the Composition C-4. The reverberated pulse of each experiment also compares well with numerical data. Figure 5 shows the best correlation between experimental and numerical results. Experimental results for Figs. 7 and 8 show slight deviations from numerical results. As mentioned, this may be due to density variation of the high explosive. A minor shift in the location of the high explosive can also have profound effects on the arrival time and magnitude of the blast load. Comparisons between experimental and numerical data deviated later in time because of venting of the vessel. Recall that Transducer 3 separated from the vessel during the first experiment thus allowing the vessel to vent for this and subsequent experiments.

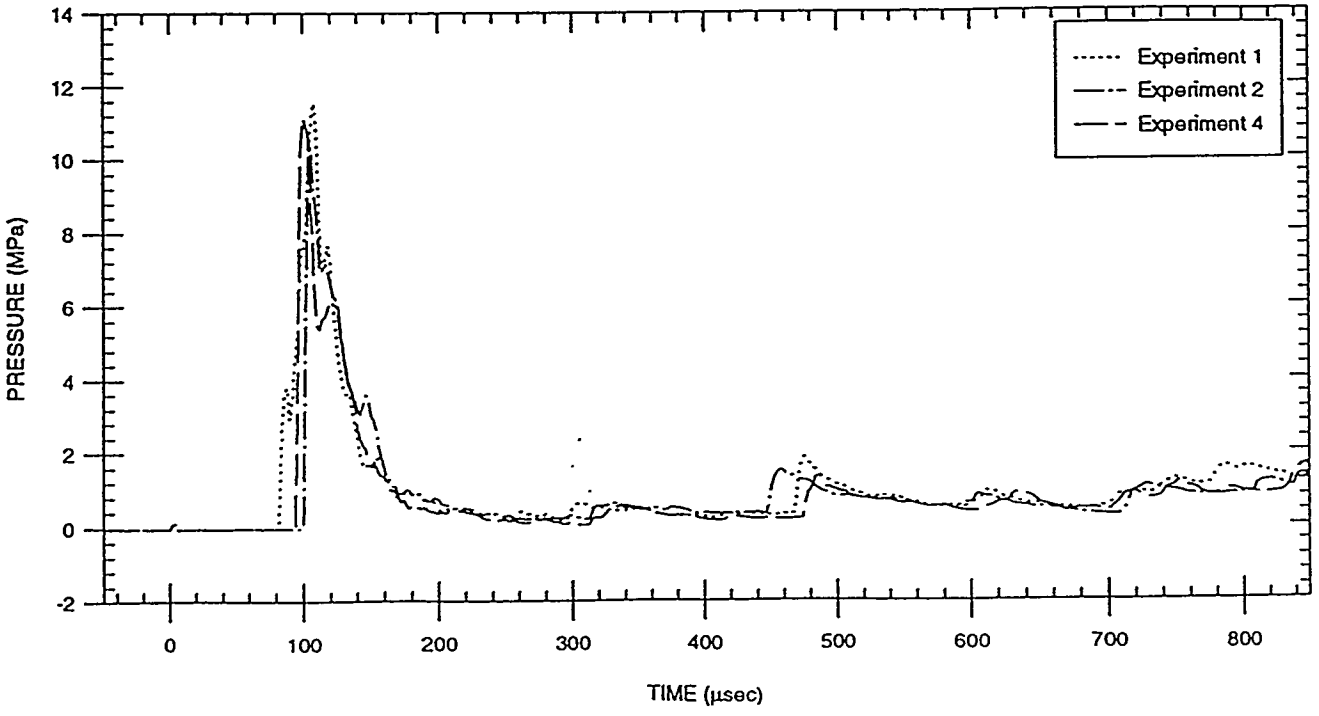

FIGURE 4. EXPERIMENTAL PRESSURE HISTORIES FOR TRANSDUCER NO. 1 (10,180°,0)

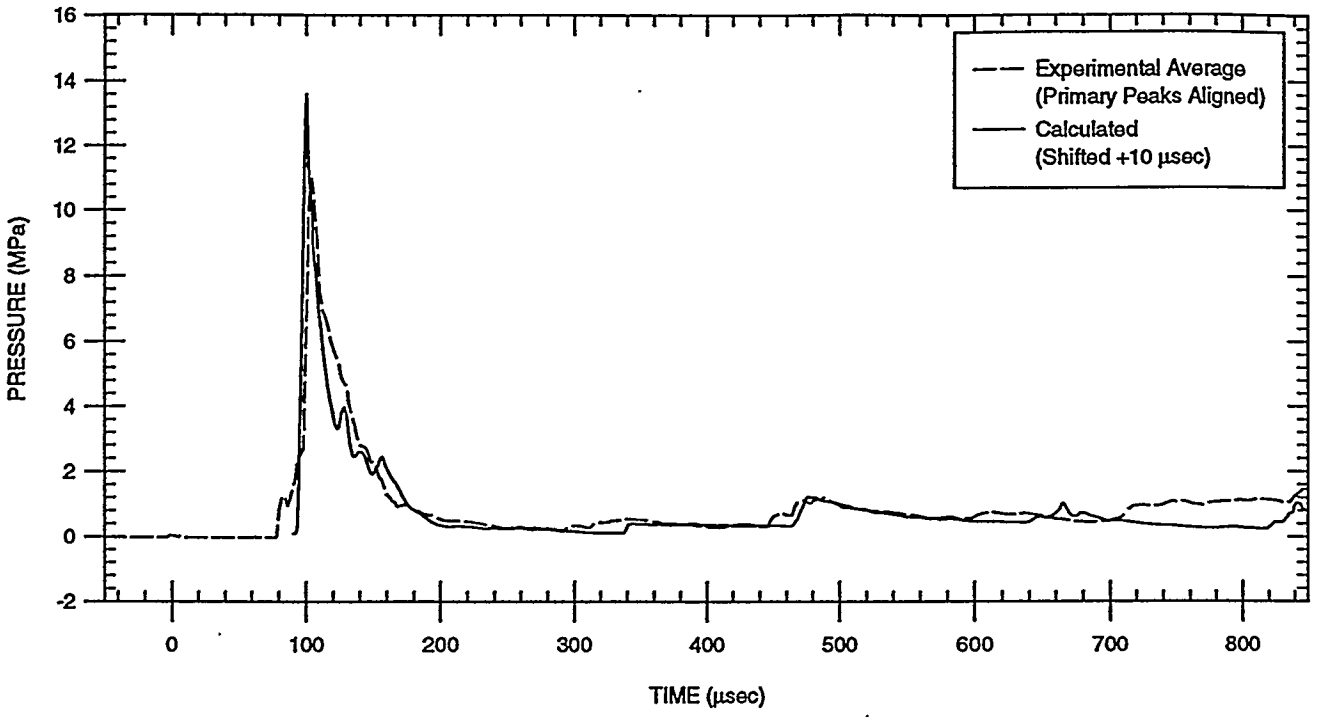

FIGURE 5. COMPARISON BETWEEN EXPERIMENTAL AVERAGE (PEAK ALIGNED) AND CALCULATED PRESSURE HISTORIES FOR TRANSDUCER NO. 1 (10,180°,0)

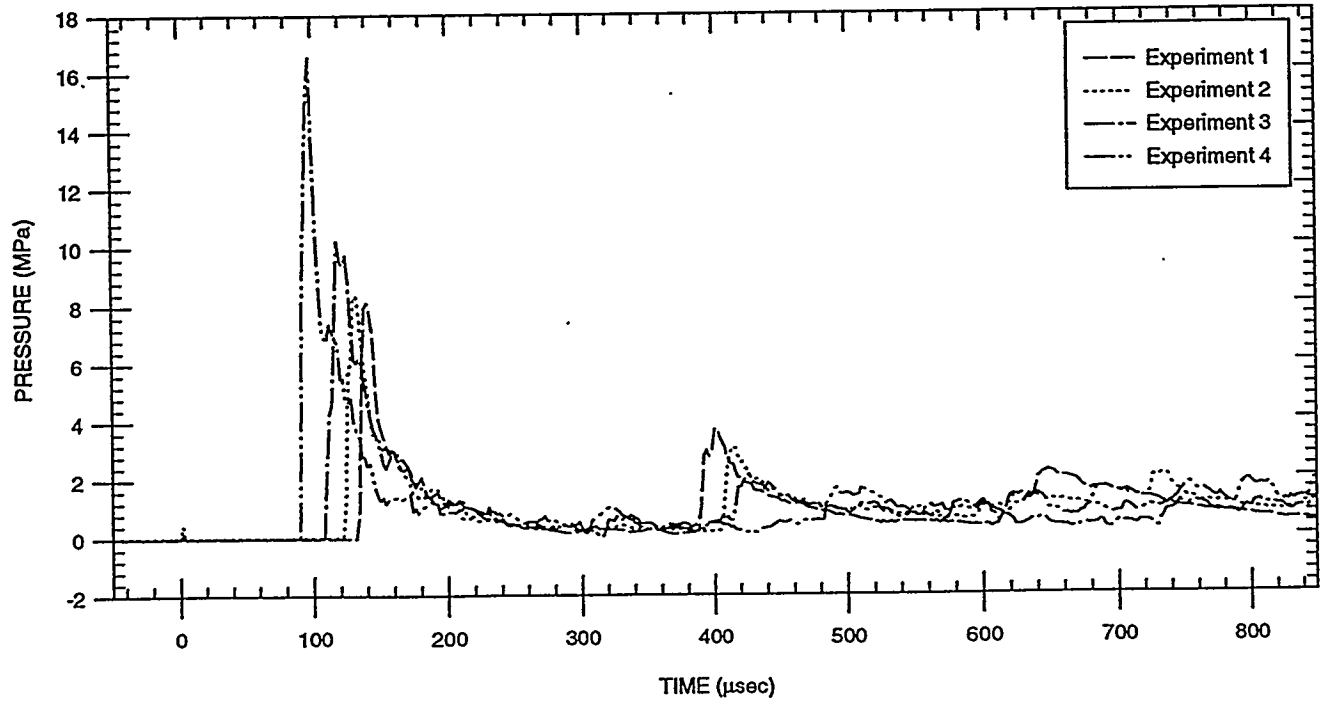

FIGURE 6. EXPERIMENTAL PRESSURE HISTORIES FOR TRANSDUCER NO. 2 (10,0°,4.87)

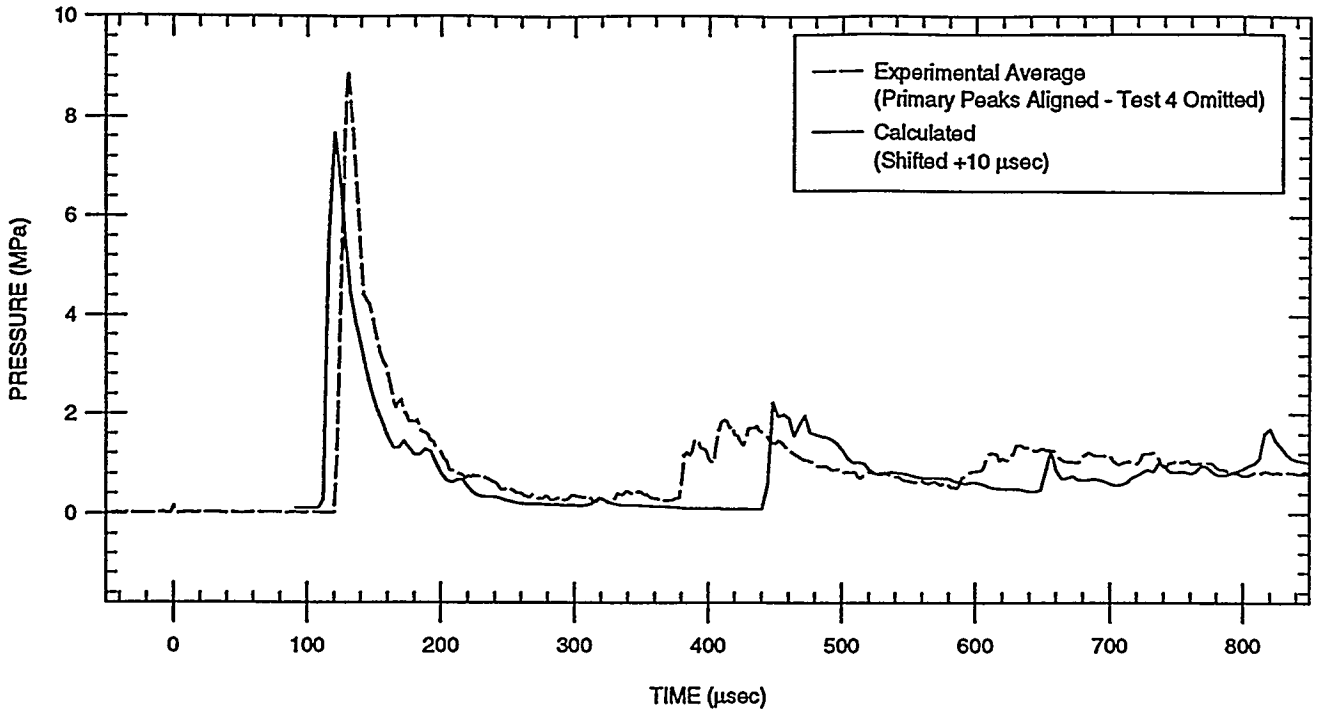

FIGURE 7. COMPARISON BETWEEN MEASURED AVERAGE(PEAK ALIGNED) AND CALCULATED PRESSURE HISTORIES FOR TRANSDUCER NO. 2 (10,0°,4.87)

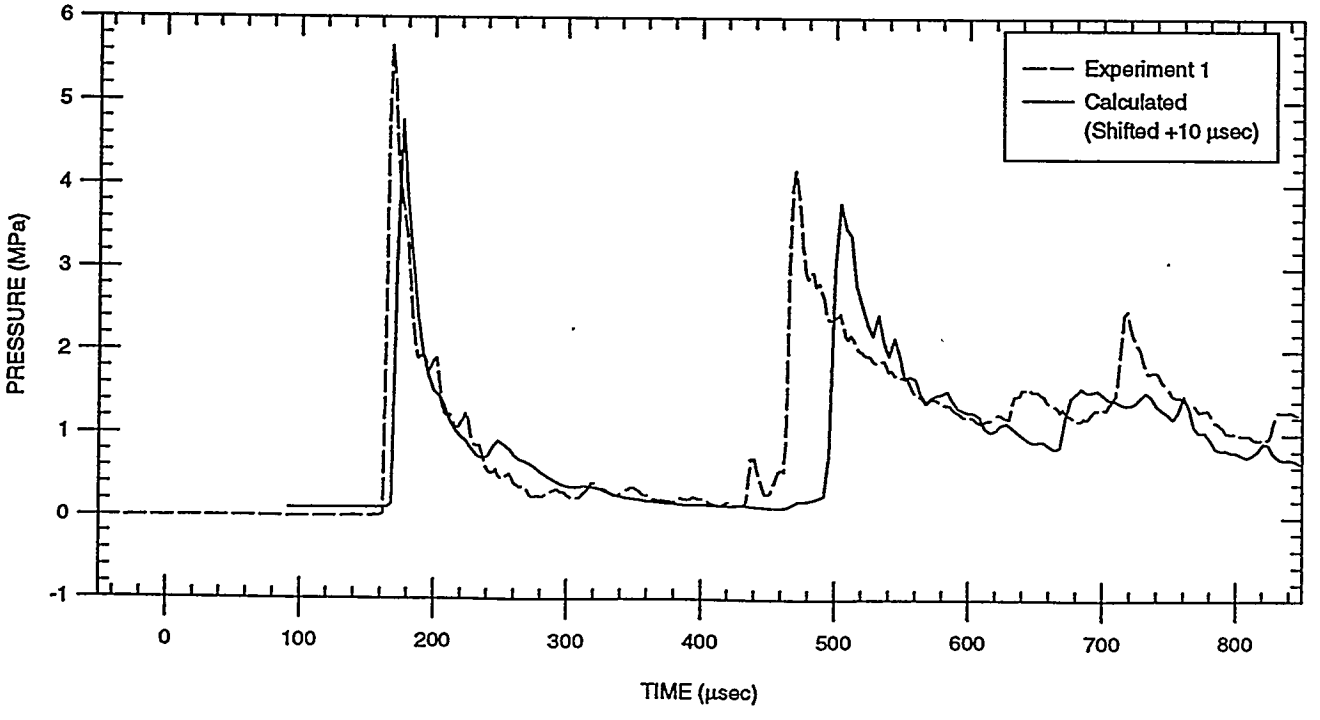

FIGURE 8. EXPERIMENTAL AND CALCULATED PRESSURE HISTORIES FOR TRANSDUCER NO. 3 (10,180°,9.75)

6.2 Biaxial Strain Gages

Figures 9 and 10 show experimental, averaged experimental, and numerical hoop strain histories for Gage 1. Figures 11 and 12 show experimental and numerical axial strain histories for Gage 1. Similarly, Figs. 13 and 14 show experimental and numerical results of hoop strain for Gage 2, while Figs. 15 and 16 show experimental and numerical axial strain histories for Gage 2. Table 4 shows maximum hoop strain, corresponding time, and natural frequency from analytical, numerical, and experimental data for Gage 1 (10,270°,0).

TABLE 4. Maximum Hoop Strain And Corresponding Time At Location (10,270°,0)

	HOOP STRAIN	TIME	NATURAL FREQUENCY
Analytical	869 μstrain	76 μsec	3300 Hz (Infinite Cylinder)
Numerical	729 μstrain	200 μsec	3205 Hz
Experimental	658 μstrain	216 μsec	3076 Hz

It is important to note that numerical strains are determined using numerical pressures (MESA-2D) and not experimental pressures. If experimental pressures are used to calculate numerical strains, better comparison with experimental strain results is likely. With this known, hoop strain histories from each experiment correlate well with numerical results. Also, analytical predictions of hoop strain compare reasonably well with both experimental and numerical results. Good correlation of natural frequency exists between analytical, numerical, and experimental data even though an infinite cylinder formulation was used to obtain the analytical natural frequency. The time where maximum hoop strain occurs correlates very well between numerical and experimental data. Analytical time, however, does deviate from both numerical and experimental data. This deviation occurs because the analytical formulation only considers the fundamental breathing mode of an infinite cylinder. Higher modes from the vessel's response are apparently playing a significant role. This reasoning also seems to account for differences in axial strain histories. Recall that the numerical model did not include the mass of the 2-in. pipe plug or any additional mass from experimental equipment (i.e., transducers, couplings, or wire connectors). It is believed that this additional mass excites higher order modes of the system and, therefore, affects the strain response. The choice of thin shell elements versus thick shell or continuum elements for the numerical model can also contribute to the response in the higher modes. Additionally, venting of the vessel, due to separation of Transducer 3, could very likely affect the reverberated blast wave and thus the strain of the vessel.

7.0 CONCLUSIONS

Correlations of analytical, numerical, and experimental data of a simple cylindrical vessel with an internal high explosive detonation are presented. Pressure transducers positioned around the vessel exhibit good comparison with numerical data. Similarly, hoop strain from both experimental and numerical results show good agreement. Axial strain correlation is less apparent. This is attributed to mass and pressure loading differences between the numerical model and the experimental system. Analysis tools like MESA-2D and DYNA-3D prove to have high value in designing containment systems subjected to internal high explosive blast loading.

Los Alamos National Laboratory is currently in the design phase of a large scale containment system for high explosive experiments. The basis of the work presented here will continue with a scaled model of the containment system shown in Fig. 17. MESA-2D pressure loading will be superimposed on a DYNA-3D finite element model. Although the system in question is truly a three-dimensional geometry, two dimensional circumferential planes exist throughout the system justifying the use of MESA-2D as a design tool. Concern of convergent shock waves due to the extensions on the vessel exists and will be evaluated accordingly. This concern, coupled with the modal response of the system, will significantly drive the design of the full scale containment system.

ACKNOWLEDGMENTS

The authors gratefully acknowledge Valgene Hart, Larry Berkbigler, Andrea Krause, Tony Cimabue, and Victor Sandoval for their contributions to this work.

REFERENCES

1. Baker, W. E., 1960, "The Elastic-Plastic Response of Thin Spherical Shells to Internal Blast Loading", ASME Journal of Applied Mechanics, Vol. 27, pp. 139-144.

2. Benham, R. A., and Duffey, T. A., 1973, "Experimental-Theoretical Correlation on the Containment of Explosions in Closed Cylindrical Vessels", Int. J. Mech. Sci., Vol. 16, pp. 549-558.

3. Proctor, J. F., 1970, "Containment of Explosions in Water-filled Right-Circular Cylinders", Exp. Mech. 10, pp. 458-466.

4. Belov, A. I., Klapovskii, V. E., Kornilo, V. A., Mineev, V. N., and Shiyan, V. S., 1984, "Dynamics of a Spherical Shell Under a Nonsymmetric Internal Pulse Loading", Fizika Goreniya I Vzryva, Vol. 20, No. 3, pp. 71-74.

5. MESA-2D Version 5, User Manual, Los Alamos National Laboratory, LA-CP-92-229, June 1992.

6. DYNA-3D User Manual, Lawrence Livermore National Laboratory, UCRL-MA-107254 Rev 1., November 1993.

7. PDA Engineering, PATRAN User Manual.

8. Blevins, R. D., 1979, "Formulas for Natural Frequency and Mode Shape", Krieger Publishing Company, p. 298.

9. Duffey, T. A., and Krieg, R., 1969, "The Effects of Strain-Hardening and Strain-Rate Sensitivity on the Transient Response of Elastic-Plastic Rings and Cylinders", Int. J. Mech. Sci., Vol. 11, pp. 825-844.

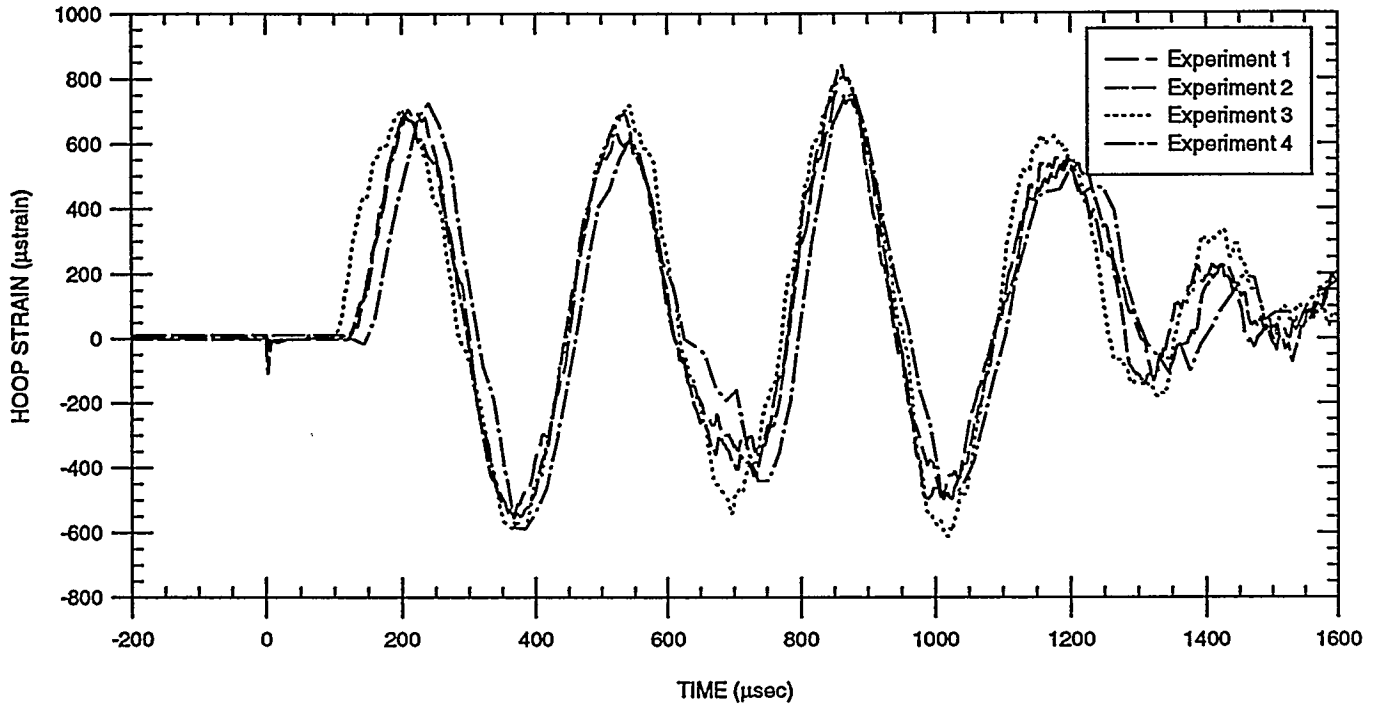

FIGURE 9. EXPERIMENTAL HOOP STRAIN HISTORIES FOR STRAIN GAGE NO. 1 (10,270°,0)

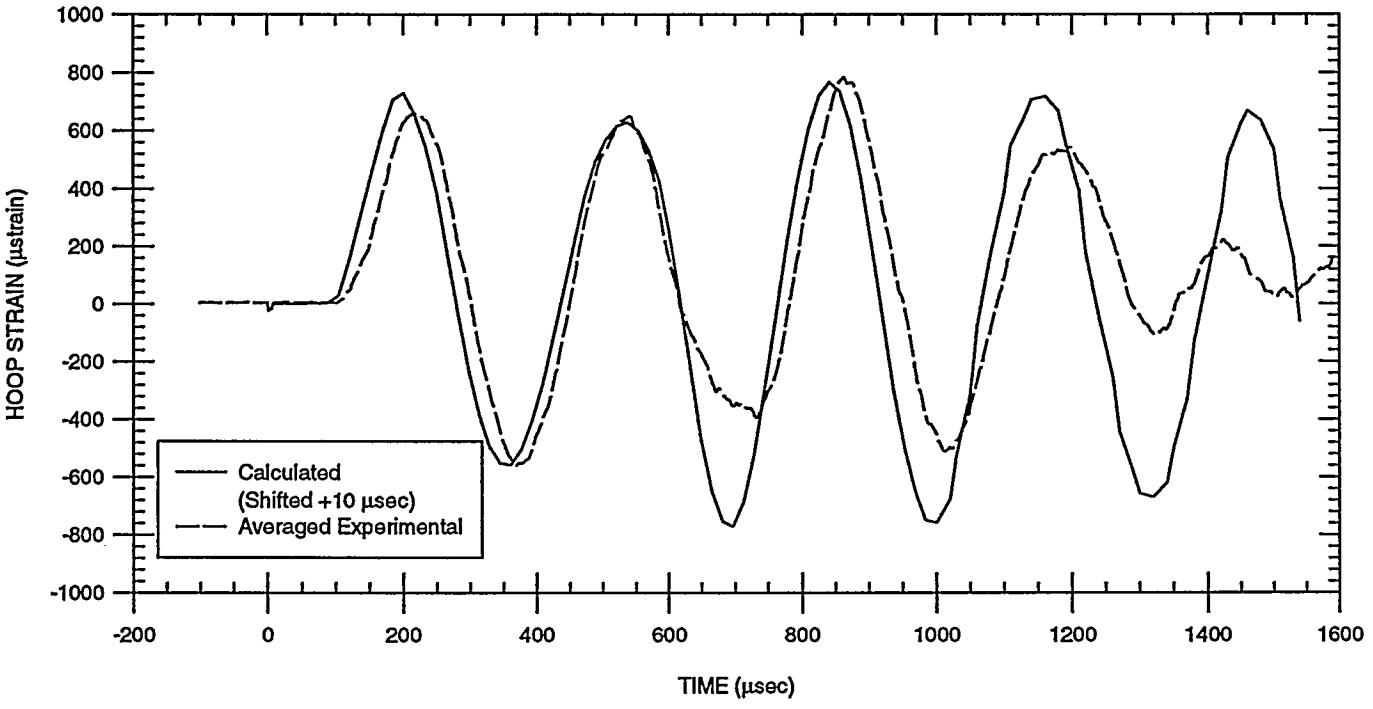

FIGURE 10. COMPARISON BETWEEN AVERAGED EXPERIMENTAL AND CALCULATED HOOP STRAIN HISTORIES FOR STRAIN GAGE NO. 1 (10,270°,0)

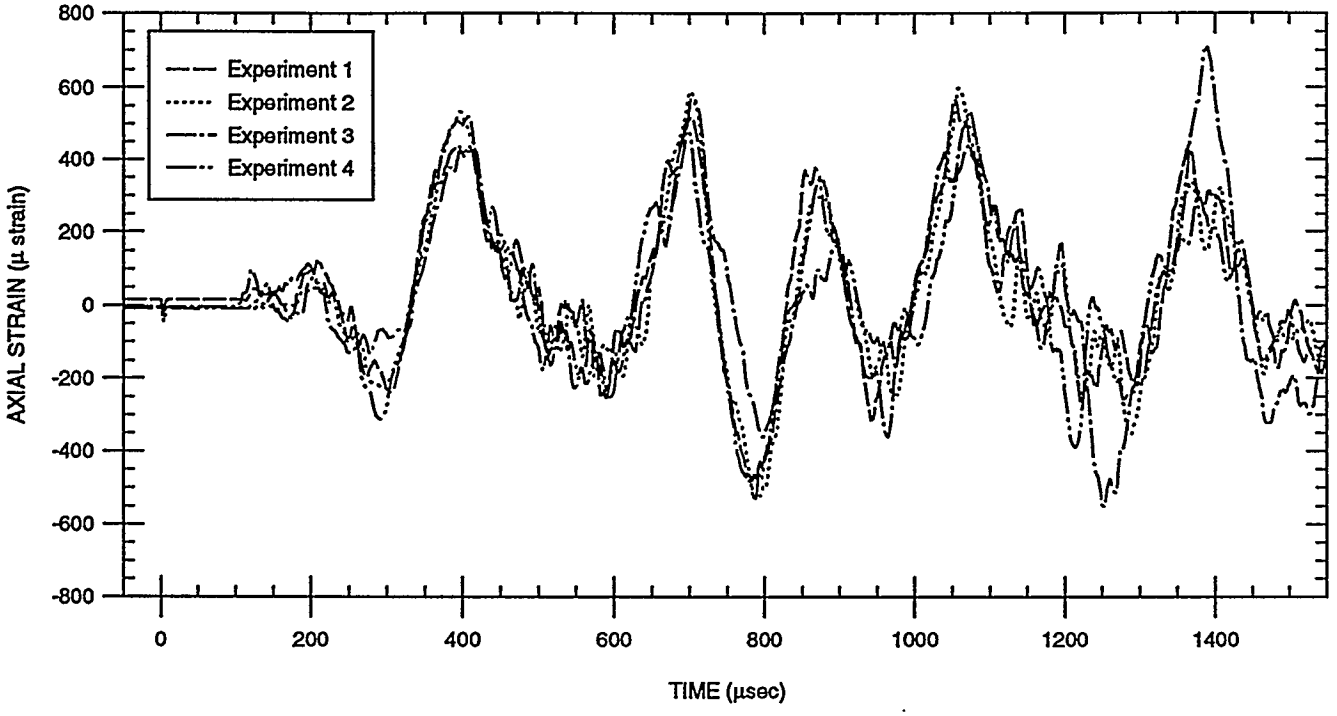

FIGURE 11. EXPERIMENTAL AXIAL STRAIN HISTORIES FOR STRAIN GAGE NO. 1 (10,270°,0)

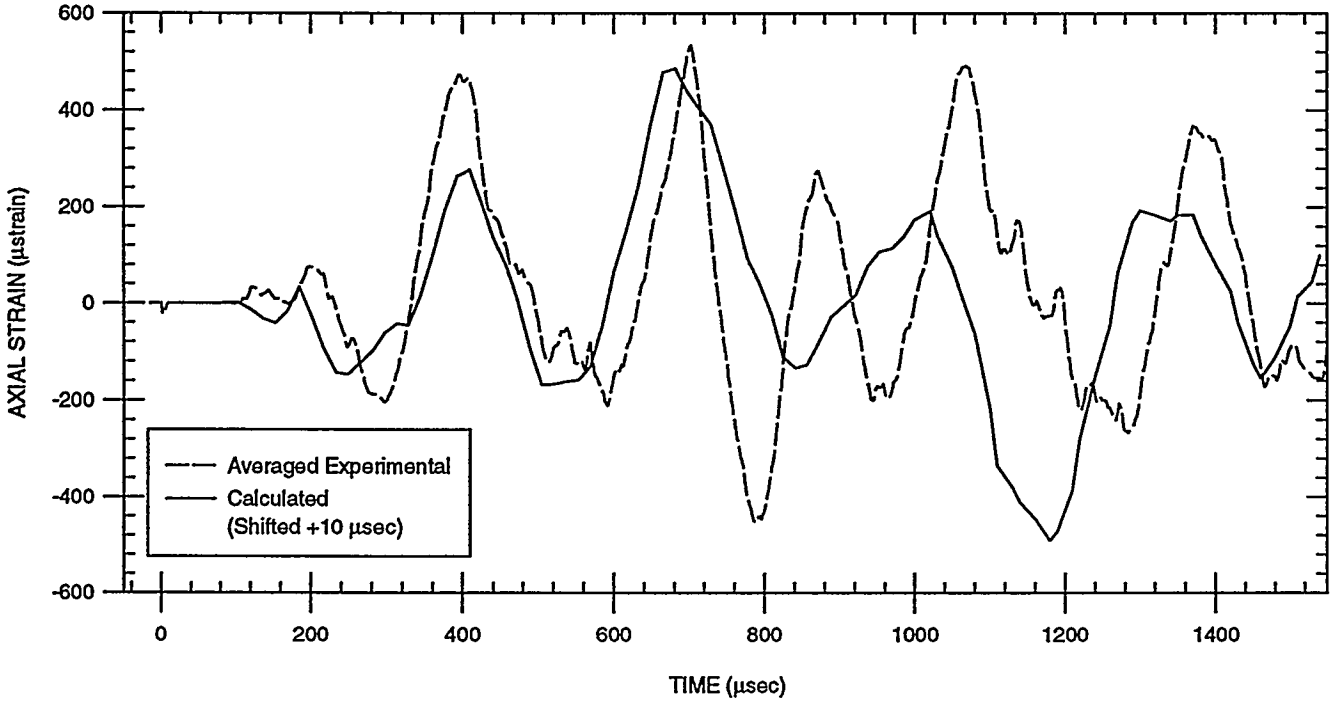

FIGURE 12. COMPARISON BETWEEN AVERAGED EXPERIMENTAL AND CALCULATED AXIAL STRAIN HISTORIES FOR STRAIN GAGE NO. 1 (10,270°,0)

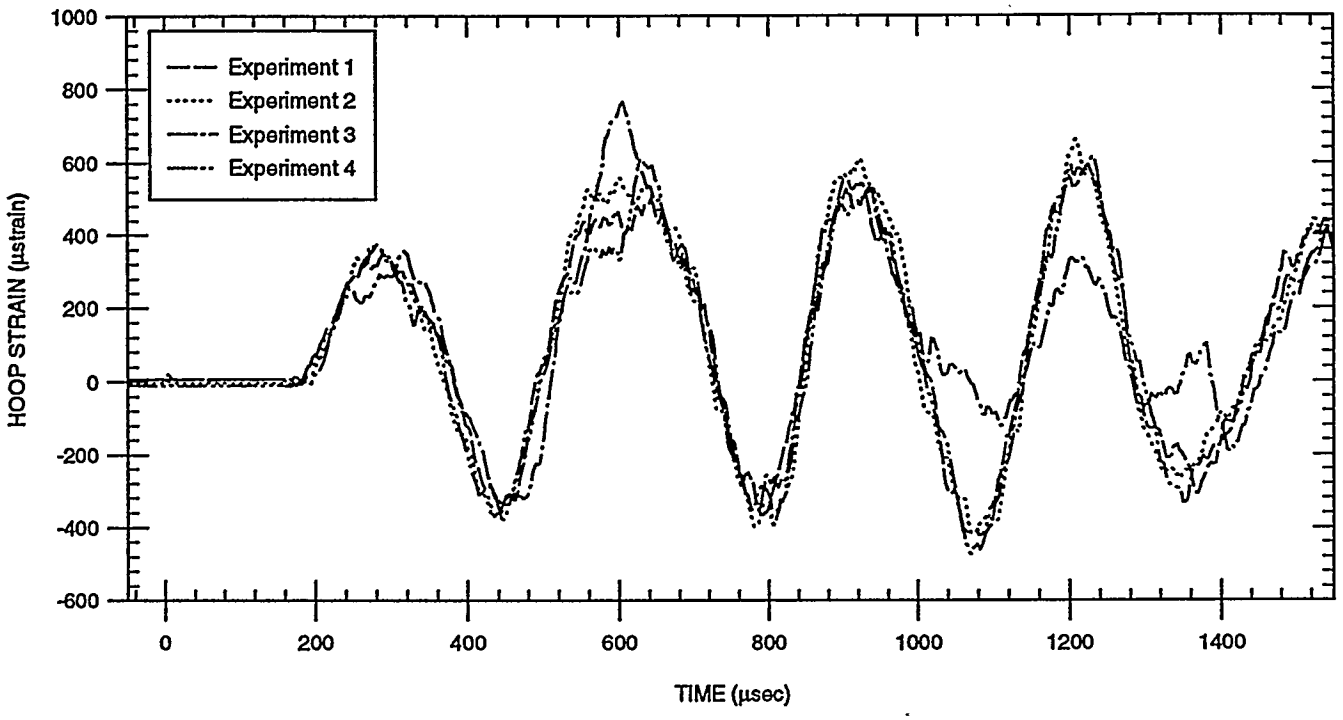

FIGURE 13. EXPERIMENTAL HOOP STRAIN HISTORIES FOR STRAIN GAGE NO. 2 (10,270°,9.75)

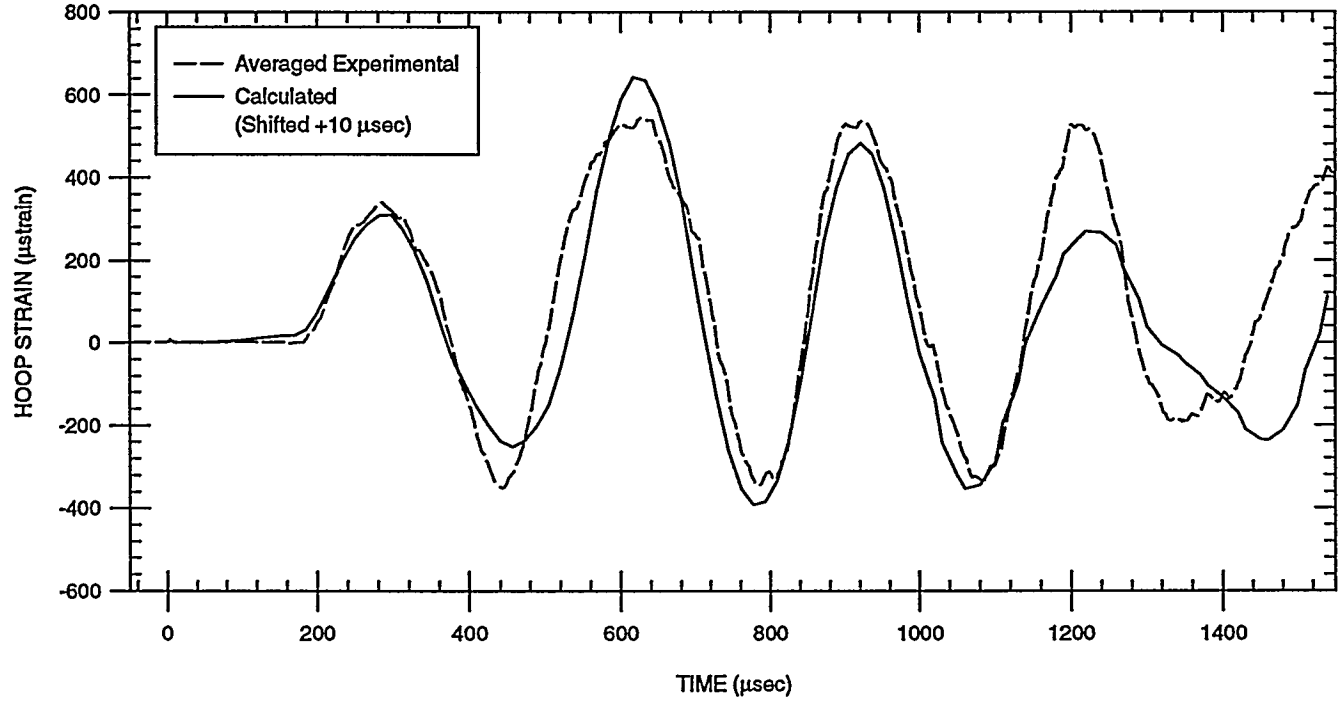

FIGURE 14. COMPARISON BETWEEN AVERAGED EXPERIMENTAL AND CALCULATED HOOP STRAIN HISTORIES FOR STRAIN GAGE NO. 2 (10,270°,9.75)

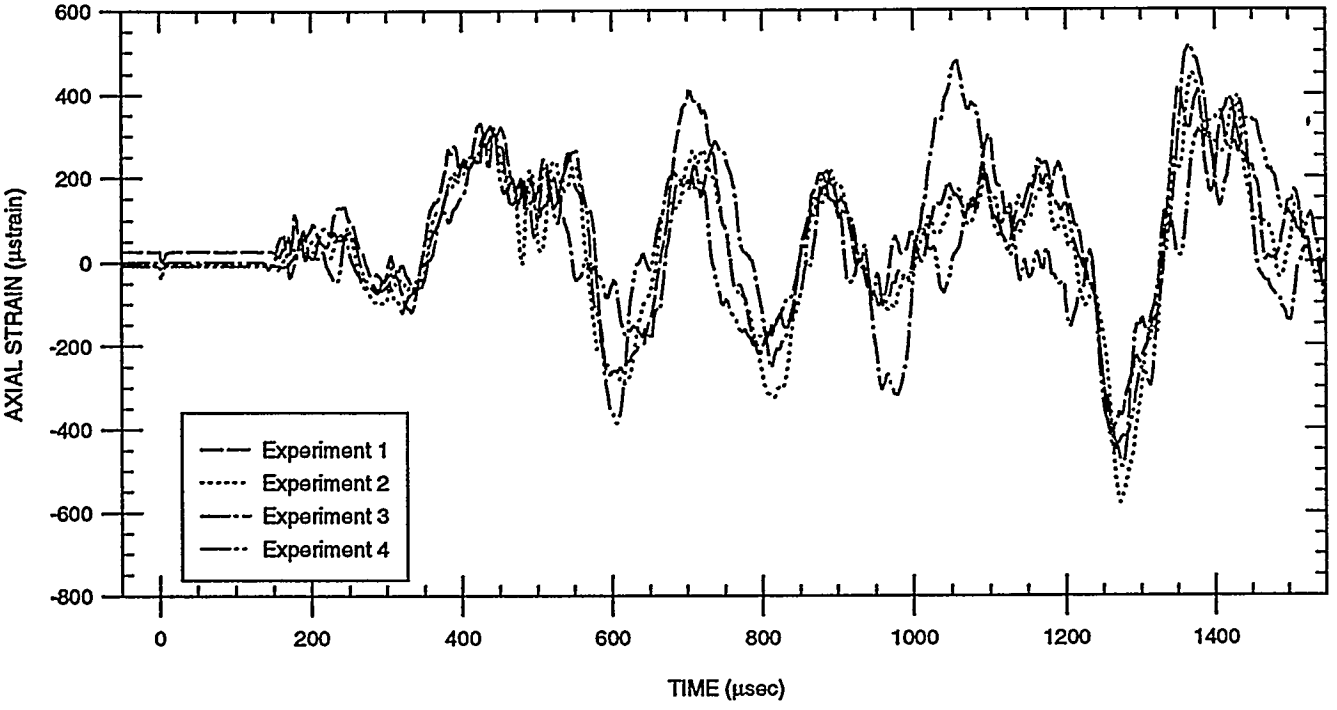

FIGURE 15. EXPERIMENTAL AXIAL STRAIN HISTORIES FOR STRAIN GAGE NO. 2 (10,270°,9.75)

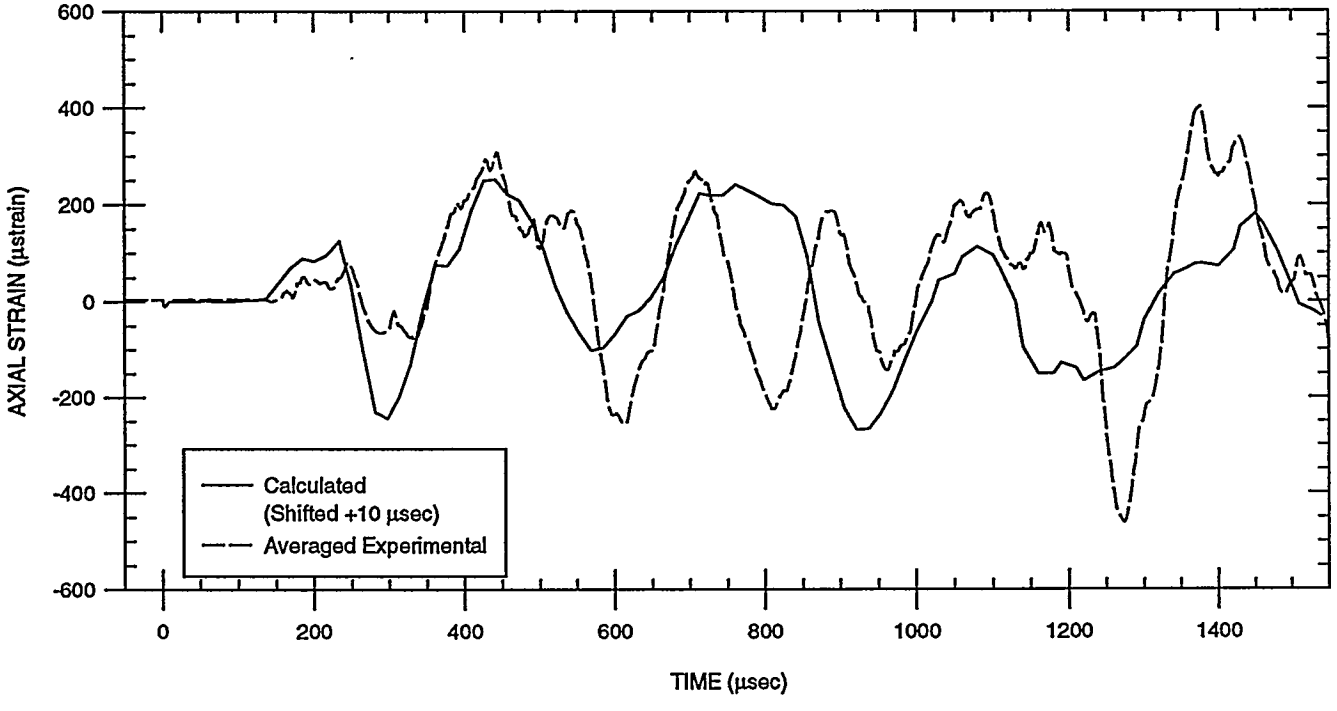

FIGURE 16. COMPARISON BETWEEN AVERAGED EXPERIMENTAL AND CALCULATED AXIAL STRAIN HISTORIES FOR STRAIN GAGE NO. 2 (10,270°,9.75)

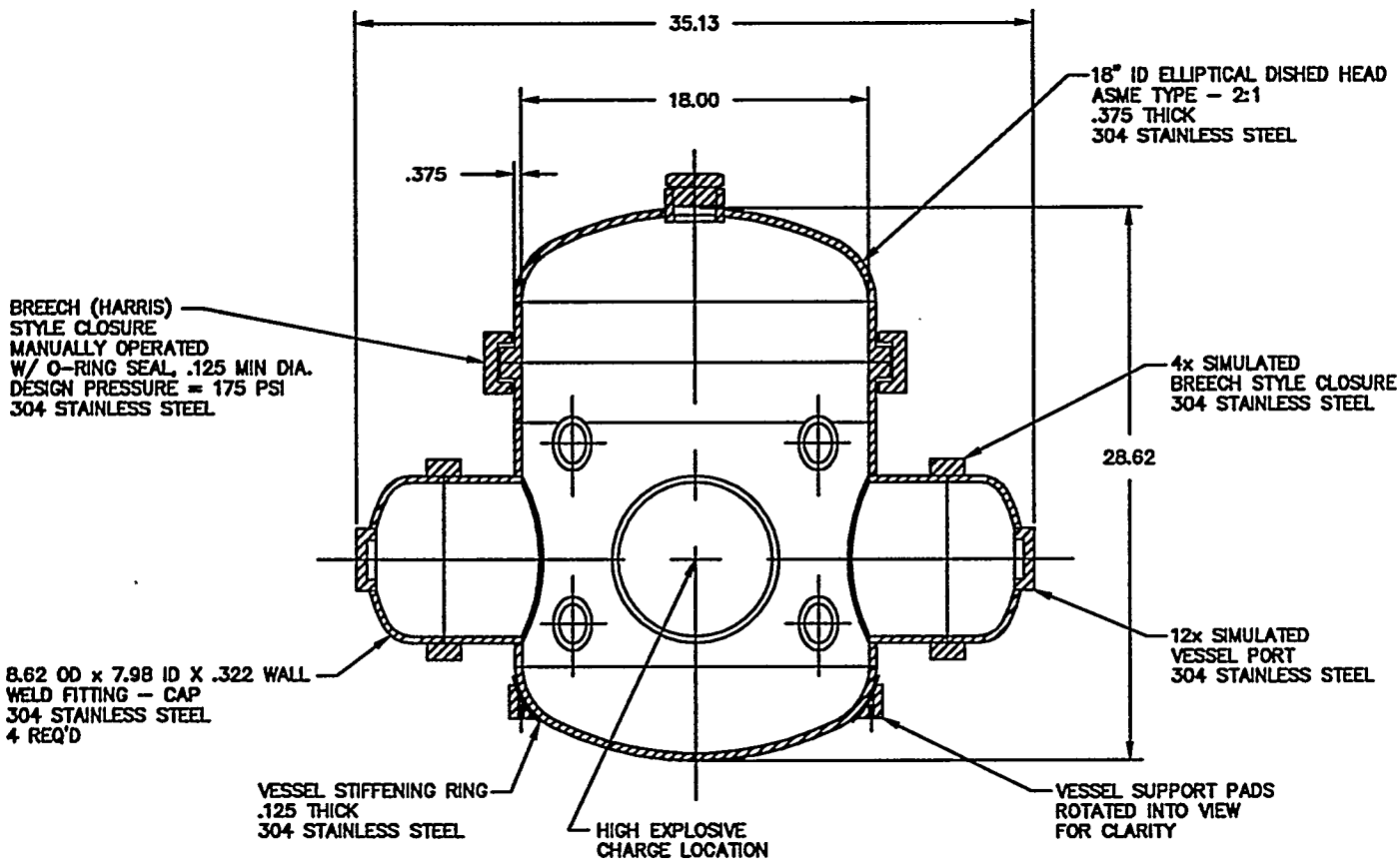

FIGURE 17. SCALED CONTAINMENT VESSEL

DISCLAIMER